More accurate fitting of ^{125}I and ^{103}Pd radial dose functions

R. E. P. Taylor[a)] and D. W. O. Rogers[b)]
Ottawa Carleton Institute of Physics, Carleton University, Ottawa, K1S 5B6, Canada

In this study an improved functional form for fitting the radial dose functions, $g(r)$, of ^{125}I and ^{103}Pd brachytherapy seeds is presented. The new function is capable of accurately fitting radial dose functions over ranges as large as 0.05 cm $\leq r \leq$ 10 cm for ^{125}I seeds and 0.10 cm $\leq r \leq$ 10 cm for ^{103}Pd seeds. The average discrepancies between fit and calculated data are less than 0.5% over the full range of fit and maximum discrepancies are 2% or less. The fitting function is also capable of accounting for the sharp increase in $g(r)$ (upturn) seen for some sources for $r < 0.1$ cm. This upturn has previously been attributed to the breakdown of the approximation of the sources as a line, however, in this study we demonstrate that another contributing factor is the 4.5 keV characteristic x-rays emitted from the Ti seed casing. Radial dose functions are calculated for 18 ^{125}I seeds and 9 ^{103}Pd seeds using the EGSnrc Monte Carlo user-code BrachyDose. Fitting coefficients of the new function are tabulated for all 27 seeds. Extrapolation characteristics of the function are also investigated. The new functional form is an improvement over currently used fitting functions with its main strength being the ability to accurately fit the rapidly varying radial dose function at small distances. The new function is an excellent candidate for fitting the radial dose function of all ^{103}Pd and ^{125}I brachytherapy seeds and will increase the accuracy of dose distributions calculated around brachytherapy seeds using the TG-43 protocol over a wider range of data. More accurate values of $g(r)$ for $r < 0.5$ cm may be particularly important in the treatment of ocular melanoma. © *2008 American Association of Physicists in Medicine.* [DOI: 10.1118/1.2964097]

I. INTRODUCTION

Many brachytherapy treatment planning systems rely on functional fits of radial dose function data when calculating the dose distribution around a brachytherapy seed. The TG-43 brachytherapy dosimetry protocol recommends using a fifth order polynomial of the form,

$$g(r) = a_0 + a_1 r + a_2 r^2 + a_3 r^3 + a_4 r^4 + a_5 r^5 \tag{1}$$

to fit radial dose functions.[1,2] Coefficients for the polynomial fit are available for many of the sources in use today. While fifth order polynomials are generally sufficient for fitting and interpolating radial dose functions over a limited range (roughly, 0.5 cm $\leq r \leq$ 10 cm), the quality of fit is often degraded when the range is extended. When the range of data is extended to include $g(r)$ values for distances less than 0.5 cm from the source, fits may suffer from a number of undesirable characteristics including nonphysical fluctuations and poor quality of fit at small radii ($r \leq 0.25$ cm). Fifth order polynomials also lack the ability to accurately represent the upturn (the change from decreasing to increasing values) in $g(r)$ seen for some seeds at distances of less than 0.1 cm.[3] Another disadvantage of using a purely polynomial function is that they generally exhibit nonphysical behavior outside of the region of fit.

A number of alternatives to fifth order polynomials are proposed by other authors including, Furhang and Anderson's double exponential,[4,5]

$$g(r) = a_0 e^{-a_1 r} + a_2 e^{-a_3 r}, \tag{2}$$

Moss's modified sigmoidal,[6]

$$g(r) = a_0 \left(\frac{a_1 + e^{a_2(r-a_4)}}{a_1 + e^{a_2(r-a_4)} + e^{a_3(r-a_4)}} \right), \tag{3}$$

and the modified fifth order polynomial from Meigooni *et al.*,[7]

$$g(r) = (a_0 + a_1 r + a_2 r^2 + a_3 r^3 + a_4 r^4 + a_5 r^5) e^{-a_6 r}. \tag{4}$$

While fits using these functions are often an improvement over fifth order polynomials, based on calculations made in this study, they are not always able to accurately fit radial dose functions over a large range of radii (e.g., 0.05 cm $\leq r \leq$ 10 cm). The value of the radial dose function at small r may be especially important when calculating the dose from eye-plaques used in the treatment of ocular melanoma.[8]

By modifying the functional form proposed by Meigooni *et al.*[7] [Eq. (4)], an improved fitting function for radial dose functions can be constructed. The new function is quite similar to the one proposed by Meigooni *et al.*, but replaces the fourth and fifth order polynomial terms with ones that vary inversely with first and second powers of r:

$$g(r) = (a_0 r^{-2} + a_1 r^{-1} + a_2 + a_3 r + a_4 r^2 + a_5 r^3) e^{-a_6 r}. \tag{5}$$

The addition of these inverse terms allows for a more rapid variation of the fitting function at small r and, hence, a much
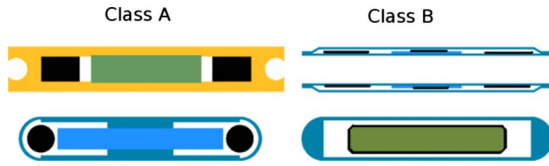
FIG. 1. Scale drawings of a few of the brachytherapy sources modeled in this study. Clockwise from the top left the sources are the [103]Pd IBt Opti-Seed 1032P, [103]Pd IBt InterSource 1031L, [125]I Amersham OncoSeed 6711, and [125]I BrachySeed LS-1. Active regions are shown in black for each source and the thickness of the active regions for the Intersource 1031L and OncoSeed 6711 are enhanced for this picture to make it visible. All four of the sources are drawn to the same scale.

better fit to radial dose function data can be achieved very close to the seed [where $g(r)$ gradients are steepest].

In this study, the EGSnrc[9,10] user-code BrachyDose[11–13] is used to calculate radial dose functions for 27 brachytherapy sources (18 ^{125}I and nine [103]Pd). A fit is performed on the radial dose function data using Eq. (5) as a target function and coefficients of the fits are tabulated. A related paper describes our EGSnrc calculated TG-43 dosimetry parameter database,[14] which provides the tabulated radial dose functions from this study as well as tables of anisotropy functions and dose-rate constants for the same sources.

II. RADIAL DOSE FUNCTION CHARACTERISTICS

Figure 1 shows scale drawings of four of the brachytherapy sources modeled in this study. For the purposes of this study, these seeds, along with other ^{125}I and [103]Pd sources, can be split into two different classes of seeds. The first class has two or more sources of radiation separated by a radio-opaque marker (Class A) and the second class has radioactive material distributed along the length of the seed including at the center (Class B). While the radial dose functions of these two classes of seeds behave roughly the same for $r > 1$ cm (decreasing monotonically), at smaller distances they behave quite differently.

Figure 2 shows radial dose functions, transverse axis dose profiles, and dose profiles parallel to, and 0.05 cm away from, the seed axis calculated in this study for two ^{125}I seeds, representative of each class of seed. The radial dose functions of the typical Class A seed (BrachySeed LS-1[15–19]) shows a trend towards zero for $r < 0.25$ cm while the typical Class B seed (OncoSeed 6711[20,21]) shows a sharp upturn in $g(r)$ for distances less than 0.1 cm from the source. Figures 2(b) and 2(c) show that the trend in $g(r)$ toward zero for Class A seeds is a result of the lack of dose along the transverse axis at small r due to the internal structure of the seed. For Class A seeds, there is a "build-up" of dose along the transverse axis as the distance from the seed increases and the two source elements emerge from the shadow of the marker. The upturn seen for Class B seeds is a result of the breakdown of the approximation of the sources as lines as well as the contribution to dose from the 4.5 keV x-rays emitted from the Ti casing as explained below.

In Rivard's study[3] of the Class B ^{125}I IPlant 3500,[3,22–24] the upturn in $g(r)$ is attributed to the breakdown of the
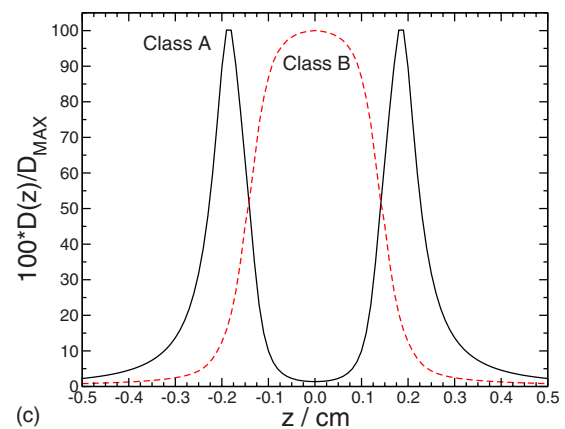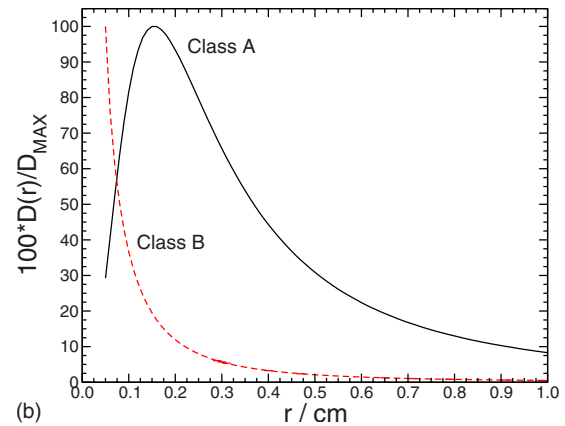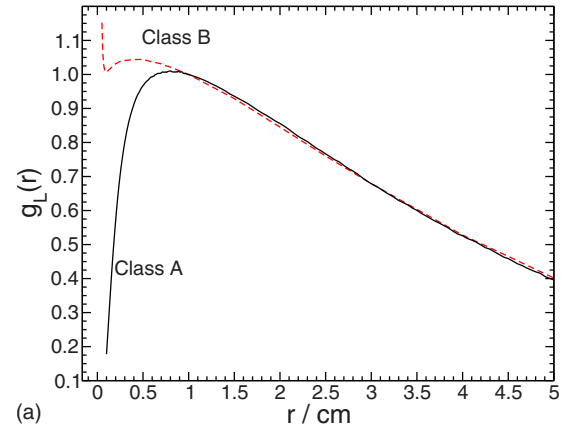

FIG. 2. Panel (a) shows typical radial dose functions, $g(r)$, for Classes A and B seeds calculated in this study. The typical Class A curves are for the [125]I BrachySeed LS-1 and the typical Class B curves are for the [125]I OncoSeed 6711. Panel (b) shows transverse axis dose profiles, without consideration of the geometry factor, for the same two seeds, and panel (c) shows dose profiles 0.05 cm away from and parallel to the seed axis. Curves in panels (b) and (c) are independently normalized to D_{max} (the maximum dose along the shown curves), so that their respective maxima are 100. The curves in panels (b) and (c) are meant to show the relative shape of the dose profiles only and not the absolute magnitude of dose.

TG-43 line source geometry function[1,2] near the seed where the distribution of radioactivity within the seed may deviate from the approximation of an ideal line source. Rivard's study demonstrates that using a more realistic Monte Carlo calculated geometry function can eliminate the upturn entirely. To illustrate this further, consider the one dimensional

analog of two ideal point sources located at $r = \pm d$, which both have $1/r^2$ dose distributions in the absence of attenuation and scatter. In this case, the one dimensional equivalent to the TG-43 line source geometry function approximation would be

$$G_{P_o}(r) = \frac{1}{r^2}, \tag{6}$$

while the actual geometry function for two point sources is

$$G_{P_{+,-}}(r) = \frac{1}{(r+d)^2} + \frac{1}{(r-d)^2}. \tag{7}$$

If we ignore any attenuation or scatter in the dose distribution, then when using Eq. (7) to calculate the radial dose function, one obtains $g_{P_{+,-}}(r) = 1$ for all r as the dose distribution is equivalent to the geometry function. However, when using Eq. (6) for the geometry function in this case, one gets:

$$g_{P_o}(r) = \frac{D(r)}{G(r)}\frac{G(r_o)}{D(r_o)} = \left[\left(\frac{1}{(r+d)^2} + \frac{1}{(r-d)^2} \right) \middle/ \frac{1}{r^2} \right] \middle/ \left[\frac{1}{(1+d)^2} + \frac{1}{(1-d)^2} \right], \tag{8}$$

which exceeds unity for $r < 1$ cm and blows up as $r \to d$ as illustrated in Fig. 3. This type of analogy can be extended to more dimensions and the same effect is seen when approximating the cylindrical sources found in many brachytherapy sources as ideal line sources.

In this paper, we show below that another factor in the upturn of $g(r)$ is the contribution to dose made by the ~4.5 keV x-rays emitted by the Ti encapsulation used for most ^{125}I and ^{103}Pd seeds. These low energy photons have a very short range in water (< 0.1 cm) and deposit all of their energy very close to the seed.

III. METHODS

III.A. Monte Carlo calculations

The EGSnrc[9,10] user-code BrachyDose[11–13] is used for all of the Monte Carlo calculations in this study. BrachyDose scores the collision kerma per history (which due to the low energies involved, can be considered equal to dose per his-

tory) in a geometric region (voxel) using a track length estimator. All calculations use photon cross sections from the XCOM[25] database and mass energy absorption coefficients are calculated using the EGSnrc user-code "g." Photon spectra recommended in TG-43U1[2] are used to sample incident photon energies and probabilities for both the ^{125}I and ^{103}Pd isotopes. Electrons are not transported and photons are transported until their energy falls below 1 keV. Up to 4×10^{10} histories are simulated in order to reduce the standard deviation (1σ) on the calculated radial dose function to 2% or less for all seeds at a distance of 10 cm from the source. A phantom size of $30 \times 30 \times 30$ cm^3 is used for all dose calculations. The voxel sizes used for scoring dose increase as the distance from the seed increase, with voxels as small as $(0.01 \text{ cm})^3$ being used for distances less than 1 cm from the center of the source. Exact details about the voxel sizes and methods used for calculating radial dose function data are identical to those found in our earlier study[13] and are not repeated here. The radial dose function, $g(r)$, is tabulated at intervals of 0.01 cm for $0.05 \leq r \leq 0.1$ cm, 0.1 cm for $0.1 < r \leq 1.0$ cm, and 0.5 cm for $5 < r \leq 10$ cm. Due to the large amount of data, the radial dose functions calculated in this study are not presented here but are available online at http://www.physics.carleton.ca/clrp/seed_database/ where they are compared to previous calculations.

Monte Carlo models of the 27 brachytherapy seeds are created using Yegin's multigeometry package,[26] which allows detailed source geometries composed of cylindrical, spherical, conical, and rectilinear objects to be modeled. All source dimensions and geometries are taken from papers by other authors and details of the source models along with references to relevant papers are included in our related TG-43 parameter database paper.[14]

To investigate the effects of x-rays emitted by the Ti encapsulation of the sources, a set of calculations is done for a few seeds in which fluorescent emissions below 5 keV are discarded immediately after they are created. The radial dose
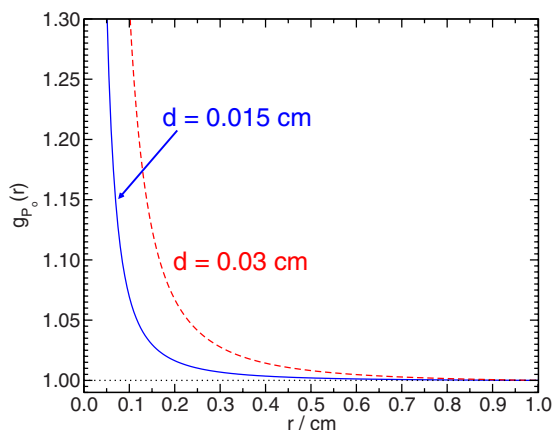
FIG. 3. Radial dose functions for two ideal point sources, with $1/r^2$ dose distributions (i.e., with no scatter or attenuation), located at $r = \pm d$. The radial dose functions are calculated using a geometry function of $G(r) = 1/r^2$ rather than the true geometry function of $G(r) = 1/(r+d)^2 + 1/(r-d)^2$.

TABLE I. Summary, for ^{125}I, of the residuals R_{avg} and R_{max} (as defined in the text) for fits using our modified polynomial, the modified polynomial of Meigooni et al., and fifth order polynomials. Fits are performed over the range of 0.05 cm $\leq r \leq$ 10 cm except for the two noted exceptions. Residuals are also shown for fits performed over the range of 0.50 cm $\leq r \leq$ 10 cm to emphasize that even for this restricted range, our modified polynomial function provides an improvement over the fifth order polynomial recommended by TG-43. All seeds are Class B except for the BrachySeed LS-1.

	Our modified polynomial				Modified polynomial of Meigooni et al.				Fifth order polynomial			
	r_{min}=0.05 cm		r_{min}=0.5 cm		r_{min}=0.05 cm		r_{min}=0.5 cm		r_{min}=0.05 cm		r_{min}=0.5 cm	
Seed name—model	R_{avg} %	R_{max} %	R_{avg} %	R_{max} %	R_{avg} %	R_{max} %	R_{avg} %	R_{max} %	R_{avg} %	R_{max} %	R_{avg} %	R_{max} %
Advantage—IA1-125A	0.35	2.2	0.29	0.97	3.0	4.0	0.27	2.6	0.70	3.1	0.40	1.3
Best I-125 -2301	0.18	1.3	0.18	1.3	0.23	5.0	0.19	1.4	0.85	3.0	0.32	1.3
BrachySeed—LS-1[a]	0.29	1.3	0.22	1.3	1.2	9.4	0.34	1.3	4.5	31	1.0	4.5
Braquibac—Braquibac	0.29	1.6	0.31	1.6	0.51	2.6	0.27	1.7	1.3	5.6	0.41	1.5
EchoSeed—6733	0.29	1.4	0.21	1.5	0.40	2.1	0.20	1.7	1.1	4.4	0.31	1.9
Implant—STM1251	0.19	1.3	0.21	1.3	0.48	1.8	0.24	1.2	1.5	5.1	0.37	1.4
InterSource—1251L[a]	0.23	1.2	0.19	1.2	1.0	8.0	0.20	1.2	2.3	19	0.43	1.9
IPlant—3500	0.22	1.3	0.21	1.1	0.33	13	0.19	1.1	1.0	7.2	0.41	1.8
IsoSeed—I25.S06	0.21	1.0	0.20	1.0	0.25	6.6	0.19	1.1	0.77	3.9	0.36	1.4
IsoSeed—I25.S17	0.25	1.4	0.21	1.3	0.30	5.0	0.20	1.1	0.89	3.6	0.32	1.4
IsoStar—IS-12501	0.30	1.3	0.30	1.4	0.66	2.2	0.29	1.4	1.7	6.7	0.45	2.1
OncoSeed—6702	0.32	1.6	0.20	1.1	0.75	29	0.20	1.1	0.82	29	0.38	1.2
OncoSeed—6711	0.22	1.7	0.22	1.7	0.30	4.2	0.22	1.7	0.79	3.1	0.36	1.8
PharmaSeed—BT-125-1	0.32	1.4	0.24	1.4	0.43	3.1	0.24	1.4	0.93	4.1	0.37	1.6
PharmaSeed—BT-125-2	0.28	1.8	0.25	1.7	0.38	3.2	0.24	1.8	0.89	3.8	0.36	2.0
Prospera—Med3631	0.24	1.2	0.18	1.2	0.48	3.8	0.17	1.1	1.6	6.6	0.36	1.4
ProstaSeed—125SL	0.32	1.9	0.22	1.6	0.38	3.5	0.22	1.6	1.1	5.6	0.53	1.9
SelectSeed—130.002	0.33	1.6	0.24	1.6	0.47	3.2	0.26	1.6	1.1	4.2	0.50	1.9
Average	0.27	1.5	0.22	1.3	0.64	6.1	0.23	1.5	1.3	8.3	0.42	1.8

[a]BrachySeed—LS-1 fit over the range of 0.2 cm $\leq r \leq$ 10 cm and InterSource—1251L fit over the range of 0.1 cm $\leq r \leq$ 10 cm.

function is recalculated using these dose distributions and compared to the standard calculation with 5 keV x-rays included.

III.B. Radial dose function fits

Radial dose functions for all of the sources are fit using Eq. (5) as the target function. Fits for fifth order polynomials [Eq. (1)] and the modified polynomial of Meigooni et al.[7] [Eq. (4)] are also calculated for comparison purposes. All fits are performed using a nonlinear least-squares fit (Levenberg-Marquardt) as implemented by the Python Scientific package (available at http://dirac.cnrs-orleans.fr/plone/software/scientificpython/). Unless otherwise indicated, all fits are performed using radial dose function data calculated in this study. An arbitrary weighting scheme is used in all fits to achieve the highest quality fit possible. In this study, the quality of a fit is characterized by its average and maximum residuals where the residuals for individual data points are defined as,

$$R_i = \frac{g_{fit}(r_i) - g_{data}(r_i)}{g_{fit}(r_i)}. \quad (9)$$

The average residual is calculated as,

$$R_{avg} = \frac{1}{N}\sum_i^N |R_i|, \quad (10)$$

and the maximum residual, R_{max} is the maximum absolute value of R_i from Eq. (9). Fits for each function are performed over the range of $r_{min} \leq r \leq r_{max}$. The value of r_{max} is set to 10 cm for all seeds while the value of r_{min} is chosen to be the smallest value possible while still maintaining average residuals of 0.5% or less and maximum residual of 2% or less. The minimum r_{min} value used in this study is 0.05 cm, as the radius of most seeds is approximately 0.04 cm. The range $0.05 \leq r \leq 10$ cm covers the clinically relevant range for ^{125}I and ^{103}Pd brachytherapy sources.

IV. RESULTS

IV.A. Radial dose function fits

For most ^{125}I seeds, an excellent fit ($R_{avg} < 0.4\%$ and $R_{max} < 2\%$) to the radial dose function is achievable over the entire range of data calculated in this study (0.05 cm $\leq r \leq 10$ cm). For most ^{103}Pd seeds, the range of r is restricted to $0.10 \leq r \leq 10$ cm in order to achieve the same quality of fit as seen for the ^{125}I seeds. The slightly restricted range for the ^{103}Pd seeds is due to the difficulty in fitting $g(r)$ for $r < 0.10$ cm for seeds whose radial dose function tend towards zero at small r (Class A seeds described above). For

TABLE II. Same as Table I except for ^{103}Pd seeds. All seeds are Class A except for the InterSource 1031L and IsoSeed Pd-103.

| Seed name—model | Our modified polynomial | | | | Modified polynomial of Meigooni et al. | | | | Fifth order polynomial | | | |
| | r_{min}=0.05 cm | | r_{min}=0.5 cm | | r_{min}=0.05 cm | | r_{min}=0.5 cm | | r_{min}=0.05 cm | | r_{min}=0.5 cm | |
	R_{avg} %	R_{max} %	R_{avg} %	R_{max} %	R_{avg} %	R_{max} %	R_{avg} %	R_{max} %	R_{avg} %	R_{max} %	R_{avg} %	R_{max} %
Advantage—IAPd-103A	0.27	1.6	0.27	1.6	1.9	21	0.33	1.7	4.3	45	0.75	4.3
BestPd-103—2335	0.34	3.0	0.32	2.8	2.1	25	0.33	2.3	5.4	53	0.96	3.9
BrachySeed—Pd-1[a]	0.31	1.7	0.28	1.7	1.7	14	0.48	2.0	4.5	31	1.9	13
InterSource—1031L	0.35	1.9	0.40	1.7	1.7	9.3	0.35	2.2	3.5	31	0.73	2.5
IsoSeed—Pd-103	0.30	2.4	0.24	2.0	0.55	2.7	0.24	2.0	1.3	10	0.50	1.6
OptiSeed—1032P	0.25	1.7	0.21	1.8	2.3	26	0.26	2.2	5.7	55	0.86	5.7
PharmaSeed—BT-103-3	0.24	1.6	0.23	1.9	2.0	23	0.26	1.7	4.2	46	0.59	3.4
Prospera—Med3633	0.37	2.1	0.35	1.8	0.85	3.2	0.38	1.8	2.0	16	0.77	2.8
TheraSeed—200	0.39	2.4	0.34	2.1	2.1	15	0.36	1.8	2.7	35	0.93	5.0
Average	0.31	2.0	0.29	1.9	1.7	16	0.33	2.0	3.7	36	0.89	4.7

[a]BrachySeed—Pd-1 fit over the range of 0.2 cm $\leq r \leq$ 10 cm due to the difficulty of fitting data very close to that seed.

the ^{125}I BrachySeed LS-1 and ^{103}Pd BrachySeed Pd-1, the range of fit is reduced to 0.20 cm $\leq r \leq$ 10 cm. Due to the geometry of these seeds, they both have nontypical behavior in their radial dose function curves for 0.05 cm $\leq r$ < 0.25 cm and including this range leads to large residuals and nonphysical behavior of the fitting function. Using the normalization of the $g(r)$ data as described in the companion paper,[14] the modified polynomial fit resulted in a function which is unity at r=1 cm and the raw data for $g(r)$ at 1 cm is within 0.4% of unity.

Tables I and II summarize the quality of fit achievable using our new function, the modified polynomial of

Meigooni et al. and fifth order polynomials for ^{125}I and ^{103}Pd seeds, respectively. The tables show the average and maximum absolute residuals for all three functions over two ranges. The first range is a larger range (0.05 cm $\leq r \leq$ 10 cm and 0.10 cm $\leq r \leq$ 10 cm for ^{125}I and ^{103}Pd seeds, respectively) while the second range is limited to 0.50 cm $\leq r \leq$ 10 cm. Fits for the latter range are included to emphasize that even for the reduced range (which encompasses the region that is probably most clinically relevant), our new functional form still offers a marked improvement over the fifth order polynomial. Average residuals of fits using the modified polynomial of Meigooni et al. are similar to

TABLE III. Radial dose function fitting parameters for ^{125}I seeds. All fits are performed over the range of 0.05 cm $\leq r \leq$ 10 cm except for the BrachySeed LS-1 and InterSource 1251L. All radial dose functions are calculated using the line source approximation with line source length given in the table. All seeds are Class B except for the BrachySeed LS-1. Raw $g(r)$ data have been normalized to give $g_{fit}(1)$=1.000.

| Seed name—model | L/cm | Fit parameters | | | | | | |
		a_0/cm^2	a_1/cm	a_2	a_3/cm^{-1}	a_4/cm^{-2}	a_5/cm^{-3}	a_6/cm^{-1}
Advantage—IA1-125A	0.300	6.7921×10^{-4}	-1.5741×10^{-2}	$1.1828 \times 10^{+0}$	2.5623×10^{-1}	-2.5011×10^{-2}	1.0344×10^{-3}	3.3650×10^{-1}
Best I-125—2301	0.395	6.4235×10^{-4}	-1.4342×10^{-2}	$1.0594 \times 10^{+0}$	4.8553×10^{-1}	-1.0204×10^{-2}	1.6721×10^{-3}	4.2050×10^{-1}
BrachySeed—LS-1[a]	0.410	-8.2908×10^{-4}	-1.5007×10^{-1}	$1.3099 \times 10^{+0}$	3.7178×10^{-1}	9.0981×10^{-3}	7.9701×10^{-4}	4.3220×10^{-1}
Braquibac—Braquibac	0.307	7.0485×10^{-4}	-2.1444×10^{-2}	$1.1969 \times 10^{+0}$	2.5892×10^{-1}	-1.9130×10^{-2}	7.4604×10^{-4}	3.4830×10^{-1}
EchoSeed—6733	0.300	5.9901×10^{-4}	-1.6969×10^{-2}	$1.1785 \times 10^{+0}$	4.2922×10^{-1}	3.0489×10^{-3}	2.5813×10^{-3}	4.6810×10^{-1}
Implant—STM1251	0.380	9.0798×10^{-4}	-2.4072×10^{-2}	$1.0947 \times 10^{+0}$	5.1514×10^{-1}	1.1439×10^{-2}	3.4677×10^{-3}	4.7100×10^{-1}
InterSource—1251L[a]	0.435	9.0016×10^{-5}	-3.8520×10^{-2}	$1.1208 \times 10^{+0}$	3.7691×10^{-1}	-2.1028×10^{-2}	9.4002×10^{-4}	3.6410×10^{-1}
IPlant—3500	0.376	1.1109×10^{-3}	-2.0318×10^{-2}	$1.1009 \times 10^{+0}$	4.5785×10^{-1}	-7.7001×10^{-3}	1.7638×10^{-3}	4.2760×10^{-1}
IsoSeed—I25.S06	0.350	6.8609×10^{-4}	-1.3642×10^{-2}	$1.0767 \times 10^{+0}$	4.3239×10^{-1}	-1.7137×10^{-2}	1.2310×10^{-3}	3.9220×10^{-1}
IsoSeed—I25.S17	0.346	7.5528×10^{-4}	-1.7660×10^{-2}	$1.1890 \times 10^{+0}$	2.7369×10^{-1}	-2.3379×10^{-2}	1.0980×10^{-3}	3.5310×10^{-1}
IsoStar—IS-12501	0.340	1.0827×10^{-3}	-3.0314×10^{-2}	$1.2465 \times 10^{+0}$	1.7819×10^{-1}	-2.2716×10^{-2}	1.0380×10^{-3}	3.1760×10^{-1}
OncoSeed—6702	0.330	1.9154×10^{-3}	-2.6413×10^{-2}	$1.1127 \times 10^{+0}$	2.9603×10^{-1}	-3.4599×10^{-2}	1.3919×10^{-3}	3.0090×10^{-1}
OncoSeed—6711	0.280	5.9638×10^{-4}	-1.3360×10^{-2}	$1.1634 \times 10^{+0}$	4.0710×10^{-1}	-5.5487×10^{-3}	1.7421×10^{-3}	4.4080×10^{-1}
PharmaSeed—BT-125-1	0.325	6.8761×10^{-4}	-1.6662×10^{-2}	$1.1849 \times 10^{+0}$	4.6299×10^{-1}	1.3971×10^{-2}	4.6737×10^{-3}	5.0110×10^{-1}
PharmaSeed—BT-125-2	0.325	4.8089×10^{-4}	-1.1519×10^{-2}	$1.1389 \times 10^{+0}$	5.0233×10^{-1}	2.7405×10^{-3}	4.4628×10^{-3}	4.9310×10^{-1}
Prospera—Med3631	0.420	8.8512×10^{-4}	-6.3400×10^{-2}	$1.1537 \times 10^{+0}$	2.9318×10^{-1}	-3.4692×10^{-2}	1.3775×10^{-3}	3.0090×10^{-1}
ProstaSeed—125SL	0.300	6.1867×10^{-4}	-1.5851×10^{-2}	$1.1656 \times 10^{+0}$	4.6505×10^{-1}	-4.1911×10^{-3}	3.6906×10^{-3}	4.7930×10^{-1}
SelectSeed—130.002	0.340	5.9991×10^{-4}	-1.4694×10^{-2}	$1.1588 \times 10^{+0}$	4.5675×10^{-1}	-3.8617×10^{-3}	3.2066×10^{-3}	4.7050×10^{-1}

[a]BrachySeed—LS-1 fit over the range of 0.2 cm $\leq r \leq$ 10 cm and InterSource—1251L fit over the range of 0.1 cm $\leq r \leq$ 10 cm.

TABLE IV. Same as Table III except for ^{103}Pd seeds fit over the range of 0.1 cm $\leq r \leq$ 10 cm. All seeds are Class A seeds except for the InterSource 1031L and IsoSeed Pd-103 seeds. Raw $g(r)$ data have been normalized to give $g_{fit}(1)=1.000$.

| Seed name—model | L/cm | Fit parameters | | | | | | |
		a_0/cm^2	a_1/cm	a_2	a_3/cm^{-1}	a_4/cm^{-2}	a_5/cm^{-3}	a_6/cm^{-1}
Advantage—IAPd-103A	0.362	-2.196×10^{-4}	-9.8072×10^{-2}	$1.8342 \times 10^{+0}$	1.2624×10^{-1}	-3.6875×10^{-2}	2.6999×10^{-3}	6.0320×10^{-1}
BestPd-103—2335	0.476	1.5101×10^{-3}	-1.3800×10^{-1}	$1.9004 \times 10^{+0}$	6.1474×10^{-2}	-2.7870×10^{-2}	2.1866×10^{-3}	5.8760×10^{-1}
BrachySeed—Pd-1[a]	0.420	1.1862×10^{-2}	-3.5324×10^{-1}	$2.2129 \times 10^{+0}$	-3.2497×10^{-1}	1.5973×10^{-2}	9.2637×10^{-10}	4.4630×10^{-1}
InterSource—1031L	0.435	2.2647×10^{-3}	-1.0300×10^{-1}	$1.8601 \times 10^{+0}$	-2.9487×10^{-2}	-2.5580×10^{-2}	2.1394×10^{-3}	5.3440×10^{-1}
IsoSeed—Pd-103	0.350	1.9287×10^{-3}	-4.7847×10^{-2}	$1.7588 \times 10^{+0}$	1.3311×10^{-1}	-4.0432×10^{-2}	2.9659×10^{-3}	5.9250×10^{-1}
OptiSeed—1032P	0.380	7.2368×10^{-4}	-1.2942×10^{-1}	$1.8649 \times 10^{+0}$	1.3182×10^{-1}	-3.7938×10^{-2}	2.6165×10^{-3}	6.0580×10^{-1}
PharmaSeed—BT-103-3	0.375	-2.0294×10^{-3}	-7.9854×10^{-2}	$1.8160 \times 10^{+0}$	1.3112×10^{-1}	-3.6732×10^{-2}	2.6985×10^{-3}	6.0500×10^{-1}
Prospera—Med3633	0.420	1.7602×10^{-3}	-1.1992×10^{-1}	$1.8106 \times 10^{+0}$	2.4745×10^{-1}	-4.9084×10^{-2}	3.5708×10^{-3}	6.3890×10^{-1}
TheraSeed—200	0.423	-3.6394×10^{-3}	-5.8095×10^{-2}	$1.9098 \times 10^{+0}$	-2.6445×10^{-1}	1.2862×10^{-2}	7.0066×10^{-11}	4.6780×10^{-1}

[a]BrachySeed—Pd-1 fit over the range of 0.2 cm $\leq r \leq$ 10 cm.

fits using our new modified polynomial over the restricted range. However, when the fits are performed over the larger range, our new function represents a large improvement over both of the other function types. It should also be noted that most of the R_{max} values from fits using our modified polynomial occur either at large r, where they are dominated by statistical uncertainties or at very small r where it is most difficult to achieve a high conformity of fit to the data. Tables III and IV give the fit parameters for our modified polynomial expression for ^{125}I and ^{103}Pd seeds, respectively.

The radial dose functions along with fits using our new function, fifth order polynomials and the modified polynomial of Meigooni *et al.* are shown for the OncoSeed 6711 in Fig. 4 and the IBt OptiSeed in Fig. 5. The inset in each figure shows the radial dose function for $r \leq 1.0$ cm. The OncoSeed 6711 data are fit over the range of 0.05 cm $\leq r \leq$ 10 cm and the OptiSeed data are fit over 0.10 cm $\leq r \leq$ 10 cm. Figure 6 shows the fit residuals for both seeds as defined in Eq. (9). From these figures, it is evident that the main strength of our

new function is its ability to fit the rapidly varying radial dose function at small distances, including the upturn in $g(r)$ seen for the Class B seeds.

IV.B. Behavior of fits for $r > r_{max}$

Since the radial dose functions are fit to very small distances from the seed using $g(r)$ from Eq. (5), there is no need to extrapolate $g(r)$ for $r < r_{min}$. However, extrapolation of the fits for $r > r_{max}$ is of some interest.[27] When estimating the radial dose function outside the range of tabulated data, the TG-43 protocol recommends using a log-linear extrapolation using data from the two largest tabulated r values.[27,28] This extrapolation technique is recommended because, for large r, $g(r)$ behaves similarly to a pure exponential curve and hence, a log-linear extrapolation can produce relatively accurate values of $g(r)$ beyond the range of tabulated data. The structure of our new function is also a good candidate for use as an extrapolation function, because the exponential part of the function dominates the polynomial factors as r increases and the behavior of the fit becomes exponential-like.
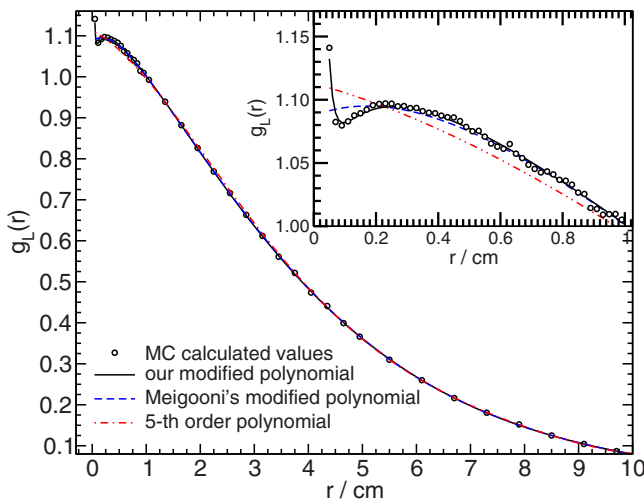

FIG. 4. Radial dose functions for the Class B ^{125}I OncoSeed 6711. The symbols represent the Monte Carlo calculated value of the radial dose function while the lines represent functional fits to the Monte Carlo values. The fit is done over the range of 0.05 cm to 10 cm. The inset figure is the same data plotted over the range of 0.05 cm to 1.0 cm.
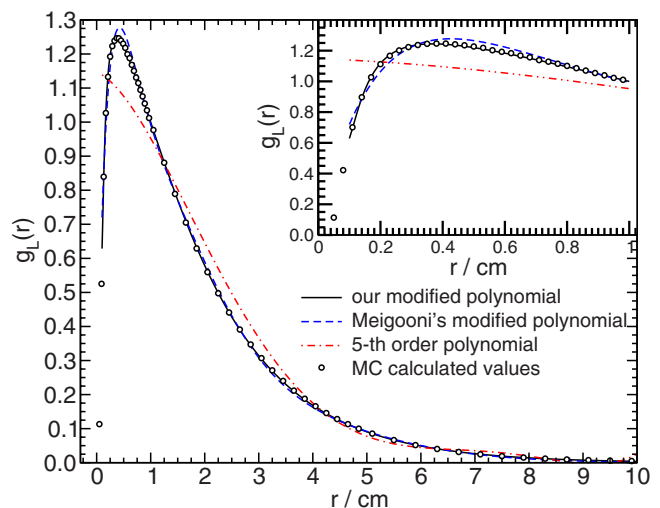

FIG. 5. Same as Fig. 4 except for the Class A ^{103}Pd OptiSeed 1032P fit over the range of 0.10 cm to 10 cm.
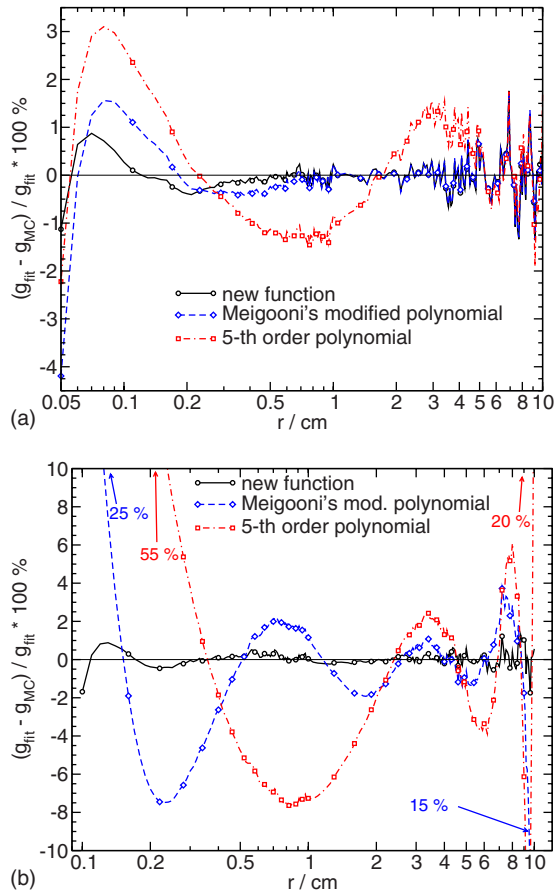
(a)

(b)

FIG. 6. Fit residuals (as defined in the text) for the three functional fits performed in this study, for (a) the [125]I OncoSeed 6711 (Class B) and (b) the [103]Pd OptiSeed 1032P seed (Class A). Residuals are calculated from the fits shown in Figs. 4 and 5. Residuals off the graph are denoted by their values and arrows.

To investigate the ability of our function to extrapolate values of $g(r)$ beyond the range of fit, radial dose functions for three ^{125}I and two [103]Pd seeds are fit over the range of 0.1 cm $\leq r \leq$ 10 cm and the resulting fits are used to calculate $g(r)$ in the range of 10 cm $< r \leq$ 14 cm. Extrapolated values are compared to Monte Carlo calculated values and values calculated using the log-linear extrapolation recommended by TG-43. The present study does not calculate dose data past $r=10$ cm, so $g(r)$ values from two other studies are used for this comparison. Data for three ^{125}I sources (Implant 1251, OncoSeed 6711, and OncoSeed 6702), are taken from a study by Kirov and Williamson[29] while data for two [103]Pd seeds are taken from studies by Monroe and Williamson[30] (TheraSeed 200) and Daskalov and Williamson[31] (IsoSeed Pd-103). Radial dose functions are available out to $r=14$ cm for these ^{125}I seeds and out to $r=14$ cm and $r=12.5$ cm for the IsoSeed Pd-103 and TheraSeed 200, respectively. For the three ^{125}I seeds and the IsoSeed Pd-103 log-linear, extrapolations are based on $g(r)$ at $r=9$ and 10 cm while values at $r=7.5$ and 10 cm are used for the [103]Pd TheraSeed 200.

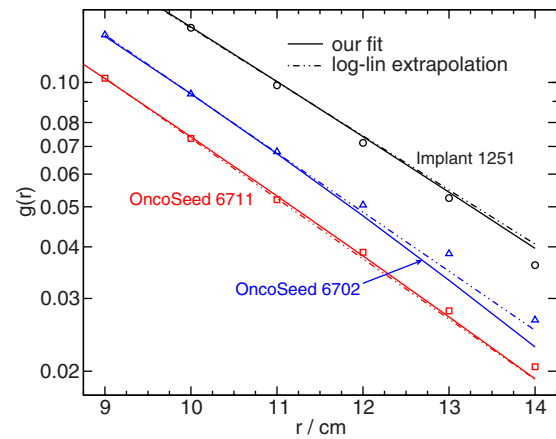Figures 7 and 8 compare $g(r)$ values calculated using Monte Carlo, our new fit function and the TG-43 log-linear

FIG. 7. A comparison of extrapolated $g(r)$ values for three ^{125}I seeds. The symbols are Monte Carlo data from Kirov and Williamson's (Ref. 29) study, while the solid lines are our fits to the same data over the range of 0.1 cm $\leq r \leq$ 10 cm. The dash-dot lines are log-linear extrapolations based on the values of $g(r)$ at $r=9$ and 10 cm. All $g(r)$ values for the Implant 1251 seed are multiplied by 1.4 for clarity.

extrapolation for the three ^{125}I and two [103]Pd seeds mentioned above. In four cases, using our fitting function from Eq. (5) for extrapolating $g(r)$ results in agreement with the Monte Carlo calculated values, which is better than or comparable to the log-linear extrapolation. For three of the seeds (Implant 1251, OncoSeed 6711, and IsoSeed Pd-103), both extrapolation methods generally result in $g(r)$ values that agree with Monte Carlo calculated values within 10% (often within 5%) for $r=11$, 12, 13, and 14 cm. For the TheraSeed, $g(r)$ at $r=12.5$ cm is underestimated by 17% and 69% by our fit function and a log-linear extrapolation, respectively. The large discrepancies for this seed may be a result of the lack of data available in Monroe and Williamson[30] for $r>5$ cm. For the OncoSeed 6702, our function underestimates $g(r)$ by

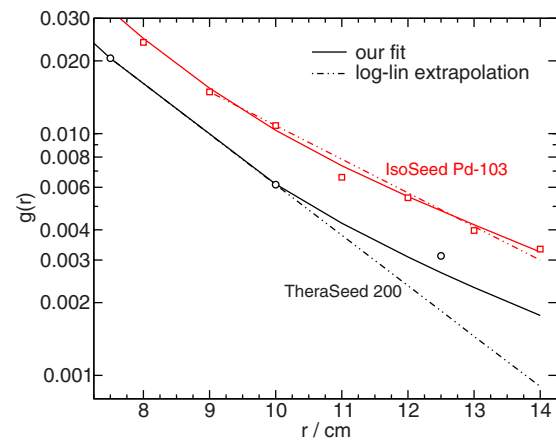
FIG. 8. Same as Fig. 7 except for [103]Pd sources. Monte Carlo data for the TheraSeed are from the study by Monroe and Williamson (Ref. 30), while Monte Carlo data for the IsoSeed Pd-103 are from Daskalov and Williamson (Ref. 31). Log-linear extrapolations are based on points at $r=9$, 10 cm for the IsoSeed Pd-103 and $r=7.5$, 10 cm for the TheraSeed. All $g(r)$ values for the IsoSeed Pd-103 are multiplied by 1.5 for clarity.
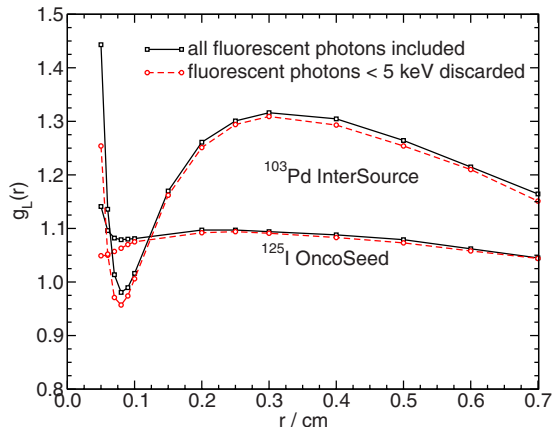
FIG. 9. Radial dose functions for the ^{125}I OncoSeed 6711 and ^{103}Pd Inter-Source 1031L. Radial dose functions are calculated both with and without the 4.5 keV characteristic x-rays from Ti. Discarding the low-energy x-rays completely suppresses the upturn in $g(r)$ for the 6711 seed. However, an upturn is still seen for the InterSource 1031L and is a result of the breakdown in the line source geometry function for small r.

16% at $r=14$ and 15 cm while the TG-43 type log-linear extrapolation underestimates $g(r)$ by only 10% and 6% at the same two distances.

The increased accuracy of extrapolation for some seeds using our function may be a result of two factors. First, the behavior of $g(r)$ is not exactly exponential in the extrapolation region and, hence, the polynomial terms in the fitting function may result in a more realistic fit function. Second, the fit function is based on the fit of many data points and is, therefore, less susceptible to statistical uncertainties than a log-linear extrapolation based on only two points. We note that this is a small sampling of radial dose function curves and more study is required to evaluate how the range of fit, quality of fit, shape of the radial dose function curve, etc. impact the accuracy of the new modified polynomial function when used to extrapolate $g(r)$ beyond the range of fit.

IV.C. Effect of low energy Ti x-rays on $g(r)$

For some ^{125}I and ^{103}Pd sources, there is an upturn in the radial dose function at distances less than 0.1 cm from the source. In his study of the ^{125}I IPlant 3500,[3] Rivard suggests that this upturn is caused by the breakdown of the TG-43 line source geometry function[1] for $r \leq L/2$ where L is the length of the line source. Rivard's study also shows that using a Monte Carlo derived geometry function, which represents the photon fluence more accurately than the line source geometry, eliminates the upturn in $g(r)$ completely. While the breakdown in the line source geometry is one factor in the upturn, the 4.5 keV characteristic x-rays emitted from the Ti casing of brachytherapy seeds are also a contributing factor.

Figure 9 shows radial dose functions calculated for the ^{125}I OncoSeed 6711 and ^{103}Pd InterSource 1031L at distances less than 1 cm from the source. Radial dose functions are shown for dose calculations made both with and without fluorescent emissions from the Ti encapsulation included. This figure indicates that for the OncoSeed 6711, the low

energy Ti x-rays, rather than the geometry function, are the primary cause of the upturn at small distances. For the Inter-Source 1031L, discarding the Ti x-rays decreases the magnitude of the upturn, but it does not change the shape very much. The upturn in the geometry function is more drastic for the InterSource 1031L than for the OncoSeed 6711 due to the different distribution of radioactivity within the seeds. While the main radiation sources for both of these seeds are cylindrical in shape, the cylindrical bands of radioactivity in the InterSource 1031L have a greater radius ($r=0.034$ cm) than the OncoSeed 6711 does ($r=0.015$ cm). The increased radius means the InterSource 1031L deviates farther from the line source approximation than the OncoSeed 6711 and, as a result of the $1/r^2$ effects explained above (also see Fig. 3), the upturn is enhanced.

It should be noted that due to the rapid decrease in dose found along the transverse axis in Class A sources for small r, there will typically not be an upturn in $g(r)$. However, the 4.5 keV photons still provide a significant dose enhancement close to the seed. The same effects are not seen for the ^{103}Pd OptiSeed, as it is encapsulated in a biocompatible polymer rather than the more commonly used titanium.

V. CONCLUSIONS

In this study, a new function for fitting radial dose functions is presented and used to fit $g(r)$ for 18 ^{125}I and nine ^{103}Pd brachytherapy seeds. The raw $g(r)$ data are available at http://www.physics.carleton.ca/clrp/seed_database/ along with an interactive calculator which gives $g(r)$ at any r for the 27 seeds reported on. Our new function gives a much higher quality of fit than the fifth order polynomial recommended by TG-43, especially when fitting radial dose function data very close to the seed. The inverse terms in our function allow for accurate fitting of radial dose function at distances of only 0.05 cm from the seed, including the upturn in $g(r)$ seen for some seeds. The upturn in the radial dose function is partially due to the low-energy x-rays emitted from the Ti casing and partly due to the breakdown of the line-source geometry function for small r. The function may also be a good candidate for extrapolation of $g(r)$ values for $r > r_{max}$, although more study is required. Overall, excellent fits to the radial dose functions of 27 different brachytherapy seeds are achieved with average discrepancies between the Monte Carlo data and the fitting function of 0.4% or less. We believe this function will make an excellent fitting function for all ^{125}I and ^{103}Pd brachytherapy seeds.

[a]Electronic mail: rtaylor@physics.carleton.ca

[b]Electronic mail: drogers@physics.carleton.ca. WWW: http://www.physics.carleton.ca/clrp/

[1]R. Nath, L. L. Anderson, G. Luxton, K. A. Weaver, J. F. Williamson, and A. S. Meigooni, "Dosimetry of interstitial brachytherapy sources: Recommendations of the AAPM Radiation Therapy Committee Task Group No. 43," Med. Phys. **22**, 209–234 (1995).

[2]M. J. Rivard, B. M. Coursey, L. A. DeWerd, M. S. Huq, G. S. Ibbott, M. G. Mitch, R. Nath, and J. F. Williamson, "Update of AAPM Task Group No. 43 Report: A revised AAPM protocol for brachytherapy dose calculations," Med. Phys. **31**, 633–674 (2004).

[3]M. J. Rivard, "Comprehensive Monte Carlo calculations of AAPM Task Group Report No. 43 dosimetry parameters for the Model 3500 I-Plant ^{125}I brachytherapy source," Appl. Radiat. Isot. **57**, 381–389 (2002).

[4]E. E. Furhang and L. L. Anderson, "Functional fitting of interstitial brachytherapy dosimetry data recommended by the AAPM Radiation Therapy Committee Task Group 43," Med. Phys. **26**, 153–160 (1999).

[5]E. E. Furhang and R. E. Wallace, "Fitting and benchmarking of dosimetry data for new brachytherapy sources," Med. Phys. **27**, 2302–2306 (2000).

[6]D. Moss, "Technical note: Improved analytical fit to the TG-43 radial dose function," Med. Phys. **27**, 659–661 (2000).

[7]A. S. Meigooni, H. Zhang, C. Perry, S. A. Dini, and R. A. Koona, "Theoretical and experimental determination of dosimetric characteristics for brachyseed Pd-103, model Pd-1, source," Appl. Radiat. Isot. **58**, 533–541 (2003).

[8]S. Awan, A. Meigooni, S. Dini, Y. Chen, F. Khan, and J. Cole, "Shortcomings in published brachytherapy source parameters for accurate dose calculation for an eye plaque implant with I-125 or Pd-103 seeds," Med. Phys. **34**, 2488–2489 (2007).

[9]I. Kawrakow, "Accurate condensed history Monte Carlo simulation of electron transport. I. EGSnrc, the new EGS4 version," Med. Phys. **27**, 485–498 (2000).

[10]I. Kawrakow and D. W. O. Rogers, "The EGSnrc Code System: Monte Carlo simulation of electron and photon transport," Technical Rep. No. PIRS-701, National Research Council of Canada, Ottawa, Canada, 2000.

[11]G. Yegin and D. W. O. Rogers, "A fast Monte Carlo code for multi-seed brachytherapy treatments including interseed effects," Med. Phys. **31**, 1771–1771 (2004).

[12]G. Yegin, R. E. P. Taylor, and D. W. O. Rogers, "BrachyDose: An EGSnrc user-code for full Monte Carlo simulation of brachytherapy implants using CT data," (unpublished).

[13]R. E. P. Taylor, G. Yegin, and D. W. O. Rogers, "Benchmarking Brachy-Dose: Voxel-based EGSnrc Monte Carlo calculations of TG-43 dosimetry parameters," Med. Phys. **34**, 445–457 (2007).

[14]R. E. P. Taylor and D. W. O. Rogers, "An EGSnrc Monte Carlo-calculated database of TG-43 parameters," Med. Phys. **35**, 4228–4241 (2008).

[15]J. F. Williamson, "Dosimetric characteristics of the DRAXIMAGE model LS-1 interstitial brachytherapy source design: A Monte Carlo investigation," Med. Phys. **29**, 509–521 (2002).

[16]R. Wang and R. Sloboda, "Monte Carlo dose parameters of the Brachy-Seed model LS-1 ^{125}I brachytherapy source," Appl. Radiat. Isot. **56**, 805–813 (2002).

[17]G. Chan and W. V. Prestwich, "Dosimetric properties of the new [125]I BrachySeed model LS-1 source," Med. Phys. **29**, 190–200 (2002).

[18]G. H. Chan, R. Nath, and J. F. Williamson, "On the development of consensus values of reference dosimetry parameters for interstitial brachytherapy sources," Med. Phys. **31**, 1040–1045 (2004).

[19]R. Nath and N. Yue, "Experimental determination of a newly designed encapsulated interstitial brachytherapy source of iodine-125-model LS-1 BrachySeed," Appl. Radiat. Isot. **55**, 813–821 (2001).

[20]J. F. Williamson, "Comparison of measured and calculated dose rates in water near I-125 and Ir-192 seeds," Med. Phys. **18**, 776–786 (1991).

[21]J. Dolan, Z. Li, and J. F. Williamson, "Monte Carlo and experimental dosimetry of an ^{125}I brachytherapy seed," Med. Phys. **33**, 4675–4684 (2006).

[22]D. Duggan and B. L. Johnson, "Improved radial dose function estimation using current version MCNP Monte Carlo simulation: Model 6711 and ISC3500 125I brachytherapy sources," Appl. Radiat. Isot. **61**, 1443–1450 (2004).

[23]D. Duggan and B. L. Johnson, "Dosimetry of the I-Plant Model 3500 iodine-125 brachytherapy source," Med. Phys. **28**, 661–670 (2001).

[24]R. E. Wallace, "Model 3500 ^{125}I brachytherapy source dosimetric characterization," Appl. Radiat. Isot. **56**, 581–587 (2001).

[25]M. J. Berger and J. H. Hubbell, "XCOM: Photon cross sections on a personal computer," Rep. No. NBSIR87-3597, NIST, Gaithersburg, MD 20899, 1987.

[26]G. Yegin, "A new approach to geometry modelling of Monte Carlo particle transport: An application to EGS," Nucl. Instrum. Methods Phys. Res. B **211**, 331–338 (2003).

[27]M. J. Rivard, W. M. Butler, L. A. DeWerd, G. S. Ibbott, A. S. Meigooni, C. S. Melhus, M. G. Mitch, R. Nath, and J. F. Williamson, "Interpolation and extrapolation methods for dosimetry algorithms," Brachytherapy **6**, 111–111 (2007).

[28]M. J. Rivard, W. M. Butler, L. A. DeWerd, M. S. Huq, G. S. Ibbott, A. S. Meigooni, C. S. Melhus, M. G. Mitch, R. Nath, and J. F. Williamson, "Supplement to the 2004 update of the AAPM Task Group No. 43 Report," Med. Phys. **34**, 2187–2205 (2007).

[29]A. S. Kirov and J. F. Williamson, "Monte Carlo-aided dosimetry of the Source Tech Medical Model STM1251 I-125 interstitial brachytherapy source," Med. Phys. **28**, 764–772 (2001).

[30]J. I. Monroe and J. F. Williamson, "Monte Carlo-aided dosimetry of the Theragenics TheraSeed Model 200 [103]Pd interstitial brachytherapy seed," Med. Phys. **29**, 609–621 (2002).

[31]G. M. Daskalov and J. F. Williamson, "Monte Carlo-aided dosimetry of the new Bebig IsoSeed [103]Pd interstitial brachytherapy seed," Med. Phys. **28**, 2154–2161 (2001).